Accepted Manuscript

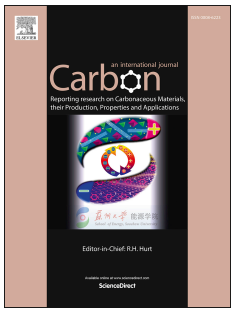

Pulsed thermal treatment of carbon up to 3000□°C using an atomic absorption spectrometer

K.J. Putman, M.V. Sofianos, M.R. Rowles, P.J.F. Harris, C.E. Buckley, N.A. Marks, I. Suarez-Martinez

PII: S0008-6223(18)30312-9

DOI: 10.1016/j.carbon.2018.03.060

Reference: CARBON 13003

To appear in: *Carbon*

Received Date: 21 November 2017

Revised Date: 1 March 2018

Accepted Date: 19 March 2018

Please cite this article as: K.J. Putman, M.V. Sofianos, M.R. Rowles, P.J.F. Harris, C.E. Buckley, N.A. Marks, I. Suarez-Martinez, Pulsed thermal treatment of carbon up to 3000□°C using an atomic absorption spectrometer, *Carbon* (2018), doi: 10.1016/j.carbon.2018.03.060.

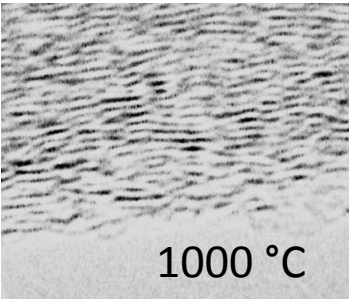

1000 °C

Conventional Furnace

t ≈ 1 hr

t ≈ 1 min

Atomic Absorption Spectrometer

3000 °C

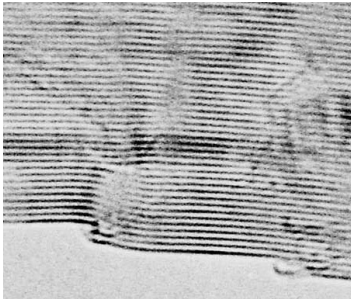

Pulsed Thermal Treatment of Carbon up to 3000 °C using an Atomic Absorption Spectrometer

K. J. Putman

Department of Physics and Astronomy, Curtin University, Perth, Australia

M.V. Sofianos

Department of Physics and Astronomy, Curtin University, Perth, Australia

M. R. Rowles

Department of Physics and Astronomy, Curtin University, Perth, Australia

P. J. F. Harris

Electron Microscopy Laboratory, Department of Chemistry, J.J. Thomson Building, University of Reading, Whiteknights, Reading, RG6 6AF, UK

C. E. Buckley

Department of Physics and Astronomy, Curtin University, Perth, Australia

N. A. Marks

Department of Physics and Astronomy, Curtin University, Perth, Australia

I. Suarez-Martinez

Department of Physics and Astronomy, Curtin University, Perth, Australia

Abstract

An atomic absorption spectrometer unit fitted with a graphite furnace module is used to perform high temperature treatment on three carbonized polymers: polyvinyl chloride (PVC), polyvinylidene chloride (PVDC) and

Email address: I.Suarez-Martinez@curtin.edu.au (I. Suarez-Martinez)

polyacrylonitrile (PAN). Using short pulses up to 45 seconds, we heat small samples to a maximum of 3000 °C. High-resolution transmission electron microscopy and X-ray diffractometry are used to track the growth of crystallites in the materials as a function of the heating temperature. We observe the well-known behavior of large crystalline graphite growth in PVC-derived samples and the formation of curved graphitic layers in PVDC- and PAN-derived samples. This graphite furnace atomic absorption spectrometer approach is an attractive alternative to conventional laboratory-scale graphite furnaces in research of high temperature treatment of carbon and other refractory materials.

1. Introduction

Graphitization of carbonaceous materials involves heating to very high temperatures in a two-step process [1]. The first step, known as carbonization, is achieved by heating material to approximately 1000 °C to drive off volatiles and increase the fraction of carbon in the sample. These temperatures can be easily achieved using standard furnaces, typically using a quartz tube and flowing argon. In the second step, known as high-temperature treatment (HTT), the sample is heated as high as 3000 °C, during which the carbon material structurally evolves and develops increasing graphitic order. The HTT process is important HTT, being used to synthesize industrially useful materials such as glassy carbon and highly-oriented pyrolytic graphite [2]. HTT of carbonaceous materials is also key to understanding basic questions in carbon science about the graphitization mechanism.

There are a number of ways of heating materials to 3000 °C, including

xenon flash lamps, pulsed laser heating and conventional graphite furnaces. The first two methods provide extremely rapid rates of heating (10^{11} K/s in the case of pulsed laser heating [3]), and the temperature of the system is not explicitly controlled. In contrast, graphite furnaces are dedicated instruments for controlled heating and use resistive heating to achieve ultra-high temperatures. Typical heating rates with laboratory graphite furnaces are of the order of tens of degrees per minute (e.g. [4, 5]), and hence it takes some hours to reach desired maximum temperatures.

There is a substantial literature using graphite furnaces for the HTT of carbon materials [1, 4, 5, 6, 7, 8], but one of the disadvantages is the high cost of this equipment. For research purposes it is attractive to find an alternative HTT method when a laboratory graphite furnace is not available. As it happens, many universities and research laboratories may already have a small graphite furnace inside certain Atomic Absorption Spectrometer (AAS) units. There are two types of AAS; flame AAS where heating up to 2600 °C is achieved using an acetylene flame, and graphite-furnace AAS (GF-AAS) where temperatures of 3000 °C are achieved by resistive heating. In this article we explore the use of a GF-AAS as an alternative to standalone graphite furnaces for the HTT of carbonaceous materials.

The GF-AAS approach differs from the traditional graphite furnace in several ways. Firstly, the GF-AAS sample heating rates are much higher, circa thousands of degrees per second. Secondly, the sample volumes are much smaller due to the geometry of the instrument. Finally, the time for each thermal cycle is restricted to less than one minute as the GF-AAS machine is not designed for continuous operation. Despite these restrictions,

we found that the GF-AAS approach is an attractive route for the study of the fundamentals of graphitization. In particular, the small sample volume is not an insurmountable problem, since many characterization techniques only require milligram amounts of material.

To demonstrate the utility of the GF-AAS approach, we study three polymers whose evolution under thermal treatment is well known: polyvinyl chloride (PVC) which graphitizes, and polyvinylidene chloride (PVDC) and polyacrylonitrile (PAN) which resist graphitization. We characterize the structures using X-ray diffraction (XRD) and transmission electron microscopy (TEM), and study the effect of temperature and residence time on the degree of graphitization. We find that all of the expected trends are observed, in particular the distinction between graphitizing behaviour with PVC, and non-graphitizing behaviour with PVDC and PAN. We describe step-by-step the methodology of using a GF-AAS to perform HTT, with the expectation that other researchers can use this approach.

2. Methodology

The workflow for carbonization and subsequent HTT is summarized by the sequence of images in Figure 1 and the temperature profile in Figure 2. Raw samples (PVC, PVDC and PAN) are placed in an alumina crucible [panel (a)] and carbonized in an argon atmosphere using an STF1200 Tube Furnace. In all cases, the heating rate is 4 °C/min, and once at 1000 °C, the temperature is held constant for an hour. After this time, the heating element is turned off and the system cools to room temperature over a period of approximately four hours. The carbonized product varies significantly between the materials: PVC produces a soft, flakey material with a shiny, black

appearance; PVDC produces a black, shiny material with a hard, foamed texture and a much larger volume than the initial sample [compare panels (a) and (b) in Figure 1]; PAN produces a hard granular material with a matte black appearance. All carbonized samples are milled into powder form using a mortar and pestle [panel (c)], with PAN being the most difficult to mill due to its hard granular texture.

To perform the HTT, a small quantity of the milled powder (milligram amounts) is transferred into a graphite tube [panel (d)] 25 mm long with an inner diameter of 3.6 mm. Samples are loaded into the tube using a small spatula, leaving a channel above the sample to permit flow of argon. The graphite tube is loaded into the GF-AAS; in our case, an Agilent GTA120 as shown in panel (e). The green box highlights the graphite tube atomizer module and the red box indicates the programmable sample dispenser which under normal operation conditions contains the solutions to be analyzed. The AAS will not operate without the liquid dispenser engaged, and so the dispenser ensemble cannot be removed. Instead, we place it on top of the instrument and allow the dispenser to operate in a dummy mode, with no samples loaded. The equipment is still supplied with a rinsing liquid which, when expelled, is captured by a waste container.

The heating regime of the furnace is controlled by software and while it allows the user to set any heating rate, the apparatus cannot operate at high temperatures for an extended time without overheating and shutting down. The GF has a supply of cooling water to remove heat from the furnace workhead. However, the AAS is not intended to maintain elevated temperatures for long period of times, and the longest time the furnace was able to be

operated at the maximum temperature of 3000 °C without triggering the thermal cutout was 45 seconds. Longer heating times were performed by consecutive pulses of 45 seconds. The heating regime is shown in red in Figure 2 and consists of 5 seconds at 100 °C, another 5 seconds at 1200 °C and then 30–45 seconds at the desired temperature. After running a few pulses, the workhead becomes noticeably hot, and at this point the unit was allowed to cool for 5-10 minutes before continuuing. In our experiments we use an Agilent instrument, but equipment from other GF-AAS manufacturers (e.g. Perkin Elmer), should be equally capable of performing in the same manner. [9]

Characterization of the samples is performed using high-resolution TEM and XRD. Specimens are prepared for TEM by grinding in an agate mortar under isopropanol, mixing in an ultrasonic bath and depositing onto lacey carbon TEM grids. Although much of the carbon deposited in this way is too thick for detailed imaging, sufficiently thin regions around the edges of particles can readily be found. The microscope is a JEOL 2010, with a point resolution of 0.19 nm, operated at an accelerating voltage of 200 kV. The current density is typically 15 pA/cm^2. To avoid beam damage, care is taken not to expose the sample to the electron beam for longer than approximately 2 minutes.

XRD is performed using a Bruker D8 Advance Diffractometer with Bragg-Brentano geometry and a Cu K-α source. XRD specimens are prepared by first placing 6 mg of powdered sample onto a low-background holder and then pressing the sample flat with a glass slide. Samples are analysed over the 2θ range from 10–90° in increments of 0.03° and a step time of 1.5 s. Patterns

are collected using a constant equatorial divergence of 0.3° with Soller slits of 2.3° in the incident and diffracted beams. Fitting is performed using fundamental parameters with instrumental broadening, Lorentz-polarisation and absorption corrected as part of the peak analysis procedure implemented in the TOPAS software [10].

A model containing the expected graphite peaks is fitted to the data, and an example fit for PVDC is shown in Figure 3. Panel (a) shows the raw data, the background model and the complete fit, while panel (b) shows the individual graphite reflections. Due to the small amount of sample, the background becomes an important part of the model for materials which are not highly graphitized. The background model was the sum of the measured background and a straight line. In some cases, including the example shown in Figure 3, large portions of the sample holder are visible to the beam, producing a small peak near 65°. When this peak is present, an additional component is added to the fitting model. The PVC samples heated to the highest two temperatures develop significant crystallinity; for these samples additional peaks appear in the data and hence the fitting model includes 101, 013, 112 and 006 reflections.

The individual peaks within the model are first fit in a symmetric manner, using a pseudo Voigt function. Some peaks showed significant asymmetry and in these cases more complex functions are used such as split-pseudo-Voigt and split-Pearson VII. The crystallite size in the c-direction (L_c) is determined using the position (θ) and full-width half-maximum (β) of the (002) and (004) peak with size in a-direction (L_a) using the (100) and (110). The cystallite sizes are calculated in the standard way via the Scherrer equation:

$$L = \frac{K\,\lambda}{\beta \cos\theta} \tag{1}$$

where λ is the wavelength of the incident X-ray beam and K is a shape factor.

In the literature it is commonplace to see L_c values calculated using $K = 0.89$, and L_a values calculated using $K = 1.84$. However, these values are largely historical. For example, the use of $K = 1.84$ for calculating L_a originates from a 1941 paper by Warren [11] and is specific to an idealized two-dimensional parallelogram. In a later 1966 paper considering a circular two-dimensional crystal, Warren and Bodenstein [12] suggest using $K = 1.77$ for L_a calculations and $K = 0.94$ for L_c calculations. Further complicating the choice, they also suggest a size-dependant shape factor for L_a varying monatomically from 1.1 to 2.0 (see Fig. 4 in Ref. [12]).

In 2004, Iwashita *et al.* [13] released a standard procedure for analysing XRD of carbon materials based on international round robin tests. Their recommendation is to assume a shape factor of unity for all crystallite shapes and sizes. This choice mitigates the problem of making assumptions about the system. In this manuscript we follow this approach and use a shape factor of $K = 1$ throughout. When comparing with literature values we rescale the reported numbers to $K = 1$.

3. Results and Discussion

One of the restrictions of using a GF-AAS is the short duration of the heating pulse. Operating the GF-AAS for too long trips a thermal cut-out and so we restrict our pulses to a maximum of 45 seconds. It is only practical

to perform a handful of pulses and hence the total heating time is significantly shorter than conventional graphite furnaces where residence times of circa 15 minutes to hours are used. To quantify the impact of using a short heating time, we perform XRD analysis on PVDC samples heated at 3000 °C for several different HTT times. Results are shown in Figure 4 where data at t=0 corresponds to the carbonized sample, while all other data corresponds to samples which undergo HTT using multiple pulses. A residence time of one minute is achieved by two pulses of 30 s, while all others are multiples of 45 s. For this material, even the shortest residence time of one minute is sufficient to achieve converged values of L_a and L_c. Were this not the case, the GF-AAS approach would not be a suitable alternative for HTT of carbon materials. As a general comment, we recommend that a similar analysis of the residence time be performed when using the GF-AAS approach. This is particularly important given that it is very difficult to assess the heat transfer path between the graphite tube and the sample. Finally, we note that for operational reasons, all TEM analysis use samples treated for 60 s, while XRD analysis use samples treated for 90 s.

The three materials studied (PVC, PVDC and PAN) were carbonized at 1000 °C, followed by HTT at three different temperatures: 2000, 2500 and 3000 °C. XRD patterns for all samples are shown in Figure 5. For all materials, the peaks become narrower and taller with temperature, indicating increasing crystallinity as temperature increases. The effect is particularly pronounced for the (002) and (004) peaks in PVC, which is expected since PVC is well-known as a graphitizing carbon, forming graphitic structures between 1700 and 3000 °C [6]. On the other hand, PVDC and PAN are non-

graphitizing carbons which do not develop a homogenous graphitic structure even at 3000 °C. While these non-graphitizing carbons do not exhibit large degrees of stacking, the presence of the basal (100) and (110) reflections indicates some level of graphenization.

Crystallite dimensions are extracted from the XRD data using equation (1) and are summarised in Table 1. For both the L_a and L_c directions, multiple peaks can be used. L_a can be determined using basal reflections such as the (100) and (110) peak. In this case, the (100) peak is more reliable than the (110) as it has a greater intensity and suffers less interference from surrounding peaks. While L_c can in-principle be determined using the (002) or (004) reflections, the (002) peak is preferred as it has a much higher intensity. Consequently, the interlayer distance, d, is extracted from the (002) peak position. Inspection of the L_c values in Table 1 also show that the values inferred from the (004) peak are typically lower, sometimes by almost a factor of two. This observation is consistent with variations in the d-spacing across the sample as noted by Houska and Warren, [14] in which broadening increases at higher angle reflections.

The crystallite size and interlayer spacing are plotted as a function of temperature in Figure 6. Following carbonization, there is little difference in L_a and L_c between the three materials; however, PVC exhibits the smallest d spacing. As temperature increases, the two non-graphitizing carbons show a small amount of graphitic growth, while PVC shows a dramatic increase in both L_a and L_c which is characteristic of graphitizing carbons [6, 15]. The interlayer spacing reduces with increasing temperatures for all materials, approaching the ultimate limit of graphite of 3.35 Å for PVC at 3000 °C.

TEM images of the three polymers are shown in Figure 7. The left column shows the samples after carbonization at 1000 °C and the right column shows the samples after HTT at 3000 °C. The images for PVC [Figure 7a) and b)] show the classic behaviour expected for a graphitizing carbon in which small oriented platelets are visible after carbonization, coalescing into large graphitic regions after HTT. Also indicated in the Figure are the values of L_a and L_c determined from XRD and these are visually consistent with the microscopy images. The images for PVDC [Figure 7c) and d)] are strikingly different, highlighting the contrast between a graphitizing and non-graphitizing carbon. Carbonized PVDC shows small, randomly oriented, platelets while the sample heated to higher temperatures contains large pores and only a few stacked layers. This appearance in TEM is consistent with our visual observations that PVDC increases its volume substantially during carbonization. This large internal porosity is hard to appreciate in Figure 7c) due to the projection nature of TEM images but it is clearly evident in Figure 7d) once graphenization has occurred. The images for PAN [Figure 7e) and f)] show another non-graphitizing carbon. The platelets are again randomly oriented in the carbonized structure and some stacking is visible after HTT.

It is interesting to note that the three carbonized materials [Figure 7a), c) and e)] have very similar values of L_a and L_c and yet the microstructure is wildly different. The platelets in the carbonized PVC sample show a clear preferential stacking, while carbonized PVDC and PAN exhibit different degrees of random orientation. This illustrates the complementary nature of the XRD and TEM techniques. Another example of the merits of combining both techniques is seen by comparing the PVDC and the PAN images. Even

though both polymers are non-graphitizing and have similar L_a and L_c values for both the higher and lower treatment temperatures the microstructure are quite different. In the case of PVDC, the porous structure seen in the TEM has a fullerenic nature [16], while the PAN structure contains twisted graphite ribbons not unlike those proposed for glassy carbons by Jenkins and Kawamura [17].

The XRD data and TEM images shows that the heating conditions achieved with the GF-AAS easily differentiate between graphitizing and non-graphitizing carbons. This is an important result, proving that the GF-AAS is a valuable technique to study graphitization. As noted in the introduction, the GF-AAS differs from conventional furnaces in several ways (heating rate, residence time and sample volume) and hence it is useful to discuss some of these differences. The effect of rapid heating on graphitizing carbons was previously studied by Okada *et al.* [18] using a conventional furnace and they observed no difference between samples heated rapidly (≈1000 °C/min, achieved by dropping the sample into the furnace) and samples additionally annealed at a slow rate (1000 °C/hr). Fair and Collins [19] studied graphitization as a function of temperature, varying the residence time from 8 minutes to 20 hours. Although the residence time had a small effect on the degree of graphitization, they concluded that graphitization was predominantly controlled by the maximum heat treating temperature. Based on this result, one would expect that our GF-AAS approach would achieve a slightly lower degree of graphitization compared to conventional furnaces.

Comparison of our data with literature values shows that for non-graphitizing carbons the GF-AAS method produces L_a and L_c values similar to those

heated using conventional furnaces. For the purpose of this discussion all literature values quoted have been scaled so that the shape factor K is 1 for all cases. Taking PVDC treated at ∼2000 °C as an example, our value of 2 nm for L_a compares to the 1.2 nm reported by Franklin [6], while our value for L_c of 1 nm compares to 0.9 nm from Franklin and 1 nm from Ban [20]. This agreement extends into higher temperatures. At 3000 °C, Franklin reports L_a and L_c values of 3 and 3.5 nm for PVDC, while we find 3 and 2 nm respectively. For PVC (i.e. a graphitizing carbon), we also find reasonable agreement for low HTT temperatures; Franklin reports 3 and 12 nm for L_a and L_c at 1720 °C, in comparison with our values of 5 and 6 nm at 2000 °C. At high temperatures the GF-AAS method achieves much smaller L_c values than conventional furnaces; Tanaike *et al.* [21] observed L_c of 180 nm for PVC at 3000 °C, while our value is just 37 nm. This lower value of L_c is entirely consistent with the time-dependent nature of the graphitization.

4. Conclusion

We demonstrate a novel approach to the high-temperature treatment of carbon materials using a Graphite Furnace Atomic Absorption Spectrometer (GF-AAS), a piece of equipment that many research institutions have. The GF-AAS is used to thermally treat three polymers up to 3000 °C for which the graphitization properties are known. We consider one graphitizing carbon (polyvinyl chloride, PVC)) and two non-graphitizing carbons (polyvinylidene chloride, PVDC, and poly-acrylonitrile, PAN). Samples are characterized using high-resolution transmission electron microscopy and X-ray diffractometry to demonstrate that the GF-AAS reproduces the same trends as a conventional graphite furnace.

Even though the amount of treated material is small (milligram quantities), and the residence times are short (circa one minute), the GF-AAS approach reproduces the expected trends and is qualitatively consistent with literature values obtained using conventional furnaces. The quantity of material produced is suitable for other common characterization techniques such as small-angle X-ray scattering, Raman and X-ray photoelectron spectroscopy. Consequently, the GF-AAS approach should be useful for any research group facing the logistical problem of heating samples to temperatures up to 3000 °C. While in this work the focus is on carbon, the methodology can equally be used to study other refractory materials where ultra-high temperatures are required.

5. Acknowledgements

This work was supported by the Australian Research Council (DP150103487). ISM acknowledges fellowship FT140100191. The authors thank Oscar Del Borrello from the University of Western Australia for his assistance in the use of the Atomic Absorption Spectrometer.

[1] A. Oberlin, Carbonization and Graphitization, Carbon 22 (6) (1984) 521–541.

[2] E. Fitzer, K.-H. Köchling, H. P. Boehm, H. Marsh, Recommended Terminology for the Description of Carbon as a Solid, Pure and Applied Chemistry 67 (3) (1995) 473–506.

[3] R. L. Vander Wal, M. Y. Choi, Pulsed laser heating of soot: morphological changes, Carbon 37 (2) (1999) 231–239.

[4] K. Kobayashi, S. Sugawara, S. Toyoda, H. Honda, An X-ray diffraction study of phenol-formaldehyde resin carbons, Carbon 6 (3) (1968) 359–363.

[5] M. B. V. Vazquez-Santos, A. Martínez-Alonso, J. M. D. Tascón, J.-N. Rouzaud, E. Geissler, K. László, Complementary X-ray scattering and high resolution imaging of nanostructure development in thermally treated PBO fibers, Carbon 49 (9) (2011) 2960–2970.

[6] R. E. Franklin, Crystallite Growth in Graphitizing and Non-Graphitizing Carbons, Proceedings of the Royal Society A: Mathematical, Physical and Engineering Sciences 209 (1097) (1951) 196–218.

[7] J. Biscoe, B. E. Warren, An X-Ray Study of Carbon Black, Journal of Applied Physics 13 (1942) 364–371.

[8] M. Monthioux, M. Oberlin, A. Oberlin, X. Bourrat, R. Boulet, Heavy Petroleum-Products - Microtexture and Ability to Graphitize, Carbon 20 (3) (1982) 167–176.

[9] Private communication with Perkin Elmer technical staff.

[10] Bruker AXS TOPAS v5 (2014).

[11] B. E. Warren, X-ray diffraction in random layer lattices, Physical Review 59 (9) (1941) 693–698.

[12] B. E. Warren, P. Bodenstein, The shape of two-dimensional carbon black reflections, Acta Crystallographica 20 (5) (1966) 602–605.

[13] N. Iwashita, C. R. Park, H. Fujimoto, M. Shiraishi, M. Inagaki, Specification for a standard procedure of X-ray diffraction measurements on carbon materials, Carbon 42 (4) (2004) 701–714.

[14] C. R. Houska, B. E. Warren, X-Ray Study of the Graphitization of Carbon Black, Journal of Applied Physics 25 (12) (1954) 1503–1509.

[15] P. J. F. Harris, New Perspectives on the Structure of Graphitic Carbons, Critical Reviews in Solid State and Materials Sciences 30 (4) (2005) 235–253.

[16] P. Harris, S. C. Tsang, High-resolution electron microscopy studies of non-graphitizing carbons, Philosophical Magazine a-Physics of Condensed Matter Structure Defects and Mechanical Properties 76 (3) (1997) 667–677.

[17] G. M. Jenkins, K. Kawamura, Structure of Glassy Carbon, Nature 231 (5299) (1971) 175–176.

[18] J. Okada, A. Sekiguchi, T. Ishii, Effect of Rapid Heat Treatment on The Properties of Carbon, The Fifth Conference on Carbon, 1961.

[19] F. V. Fair, F. M. Collins, Effect of Residence Time on Graphitization at Several Temperatures, The Fifth Conference on Carbon, 1963.

[20] L. L. Ban, D. Crawford, H. Marsh, Lattice-Resolution Electron-Microscopy in Structural Studies of Non-Graphitizing Carbons From Polyvinylidene Chloride (Pvdc), Journal of Applied Crystallography 8 (AUG1) (1975) 415–420.

[21] O. Tanaike, M. Inagaki, Effect of ether coordination for sodium intercalation into poly(vinyl chloride) cokes with different graphitization degree, Synthetic Metals 96 (2) (1998) 109–116.

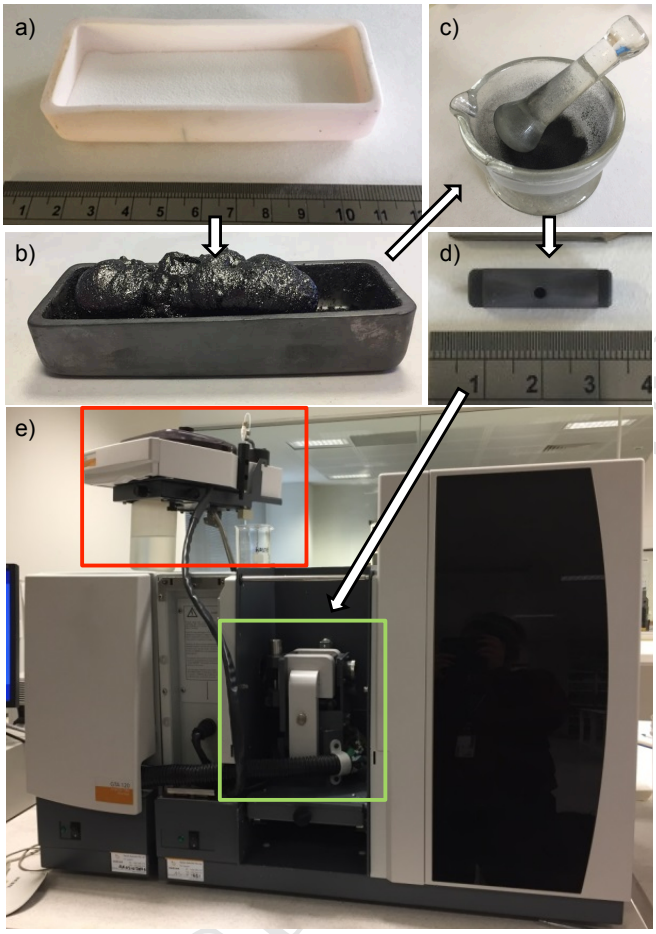

Figure 1: a) Raw PVDC in an Al_2O_3 crucible. b) PVDC after carbonization at 1000°C for an hour. (c) Mortar and pestle with ground carbonized PVDC. (d) Graphite tube, units in the ruler are cm. (e) Atomic Absorption Spectrometer with a graphite tube atomiser. The furnace assembly is indicated in green box. Red box indicates the programmable sample dispenser which has been set aside.

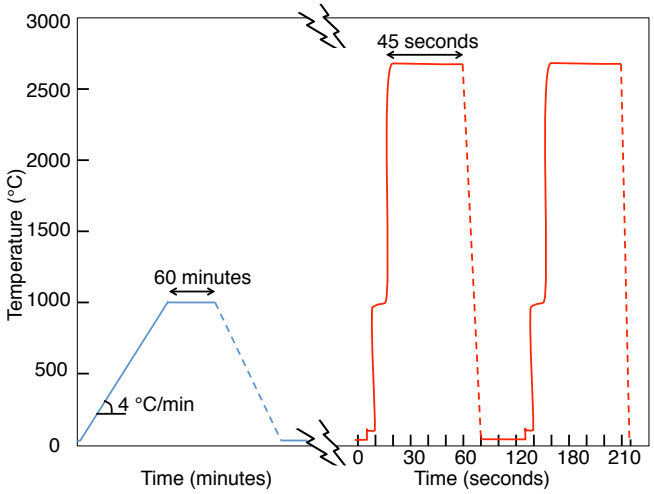

Figure 2: Heating regime for carbonization (blue lines; performed in a tube furnace) and subsequent HTT (red lines; performed in the GF-AAS). The carbonization process takes many hours, while the HTT takes around a minute. Typically, two HTT pulses are used as depicted. Dotted lines indicate cooling to ambient once the heating element is switched off.

Sample	Temp (°C)	L_c (nm) (002)	(004)	L_a (nm) (100)	(110)	d (Å)
PVC	1000	2.0	1.5	1.5	1.8	3.44
	2000	6.0	3.1	4.7	3.7	3.43
	2500	20.5	10.1	5.7	3.8	3.40
	3000	37.8	17.5	22.2	31.3	3.38
PVDC	1000	0.9	0.6	1.9	1.6	3.67
	2000	1.1	1.3	1.6	1.6	3.63
	2500	1.4	1.0	2.5	2.5	3.54
	3000	2.1	1.6	3.4	2.3	3.46
PAN	1000	1.3	0.6	2.1	1.7	3.50
	2000	1.8	0.8	2.7	2.4	3.49
	2500	2.4	1.0	3.6	2.1	3.46
	3000	2.9	1.6	3.8	3.2	3.43

Table 1: Crystallite size and interlayer spacing obtained from XRD analysis as a function of heat-treatment temperature for the three polymers. Values for L_a are derived from (100) and (110) peaks, while values for L_c are derived from (002) as well as from (004). The value of d is obtained from the position of the (002) peak.

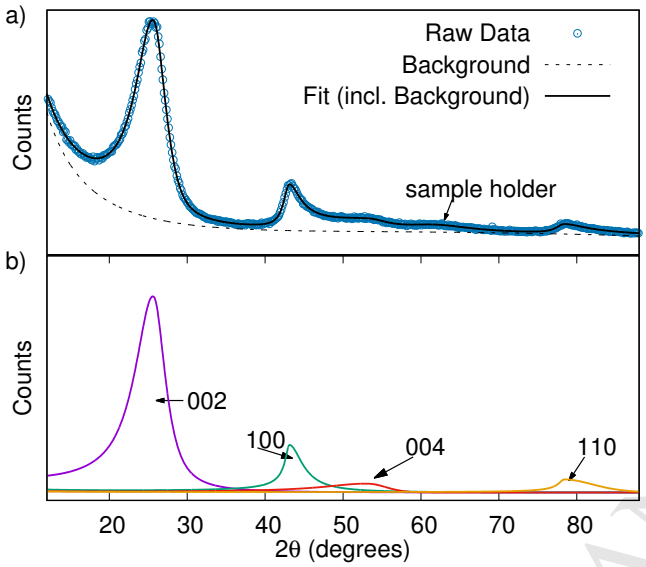

Figure 3: Example of the fitting procedure for the XRD data, using data from both PVC and PVDC, heated for 90 s at 3000 °C. Raw data is shown by circles for the PVC a) and PVDC b) with background is shown by dotted line and the complete fit is shown by a solid line; individual graphite reflections within the fitting model are seen in c) PVC and d) PVDC.

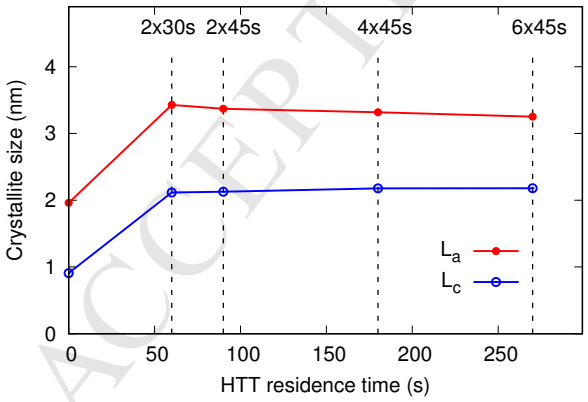

Figure 4: Variation of L_a and L_c in PVDC as measured using XRD as a function of the HTT residence time. Heating is performed at 3000 °C using multiple pulses as indicated in the figure.

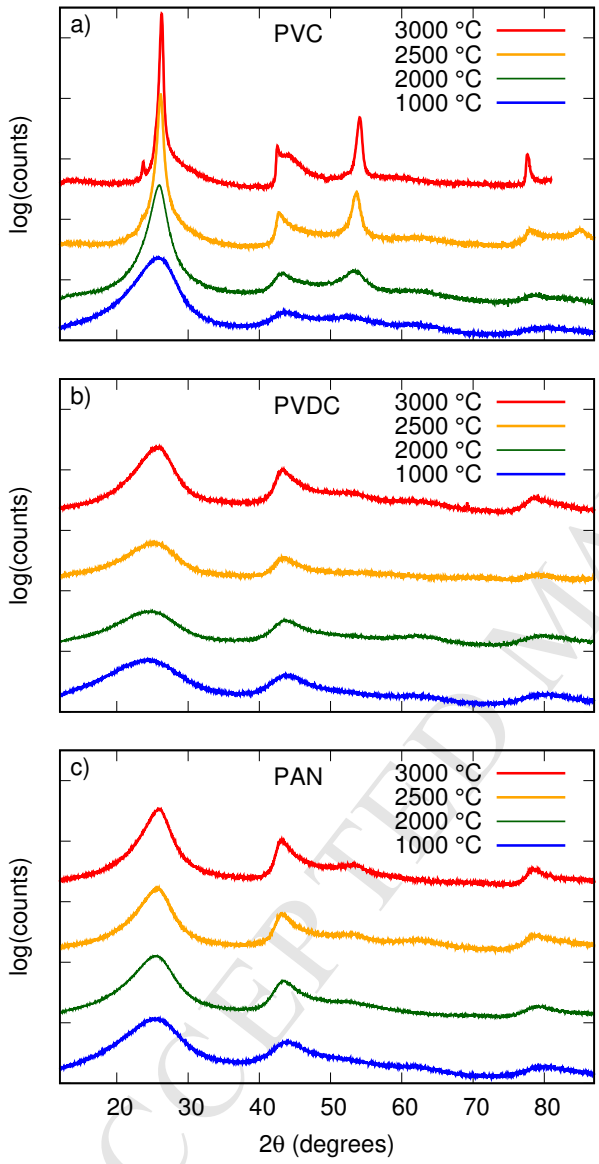

Figure 5: X-ray diffraction patterns for a) PVC, b) PVDC, and c) PAN, carbonized at 1000 °C with subsequent HTT at the temperatures indicated. Data is shown on a logarithmic scale and successive temperatures are offset vertically for clarity. All data is shown with the background removed.

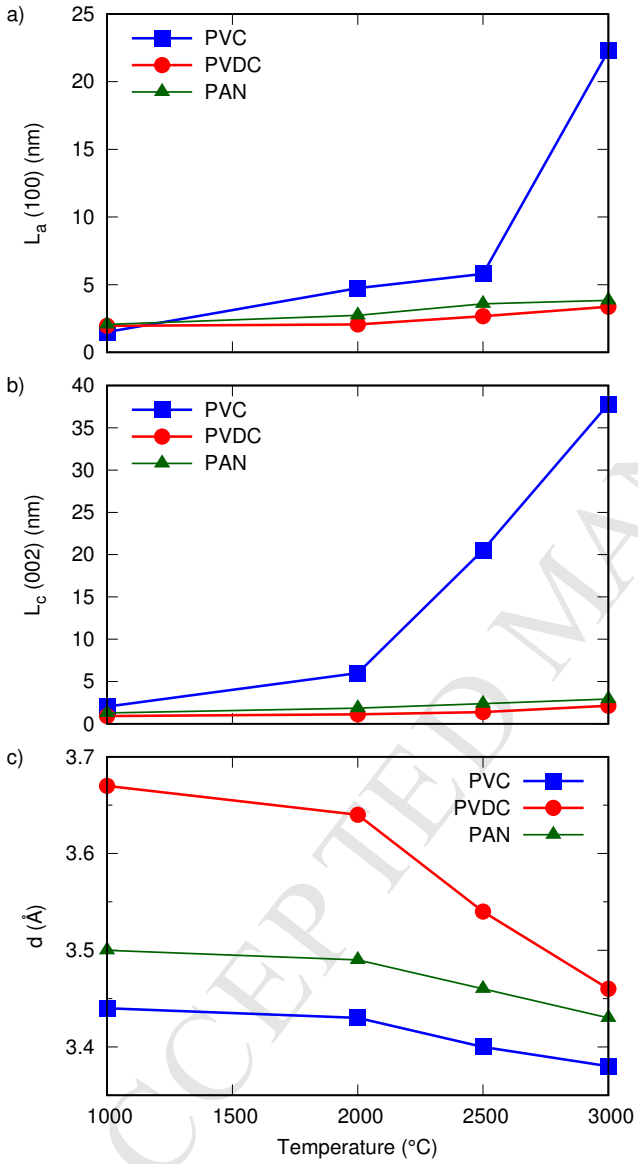

Figure 6: Plots showing the crystallite size and interlayer spacing as a function of temperature for the materials. a) L_a is reported from the (110) peak, b) L_c is reported from the (002) peak and c) interlayer spacing as differ from the position of the (002) peak.

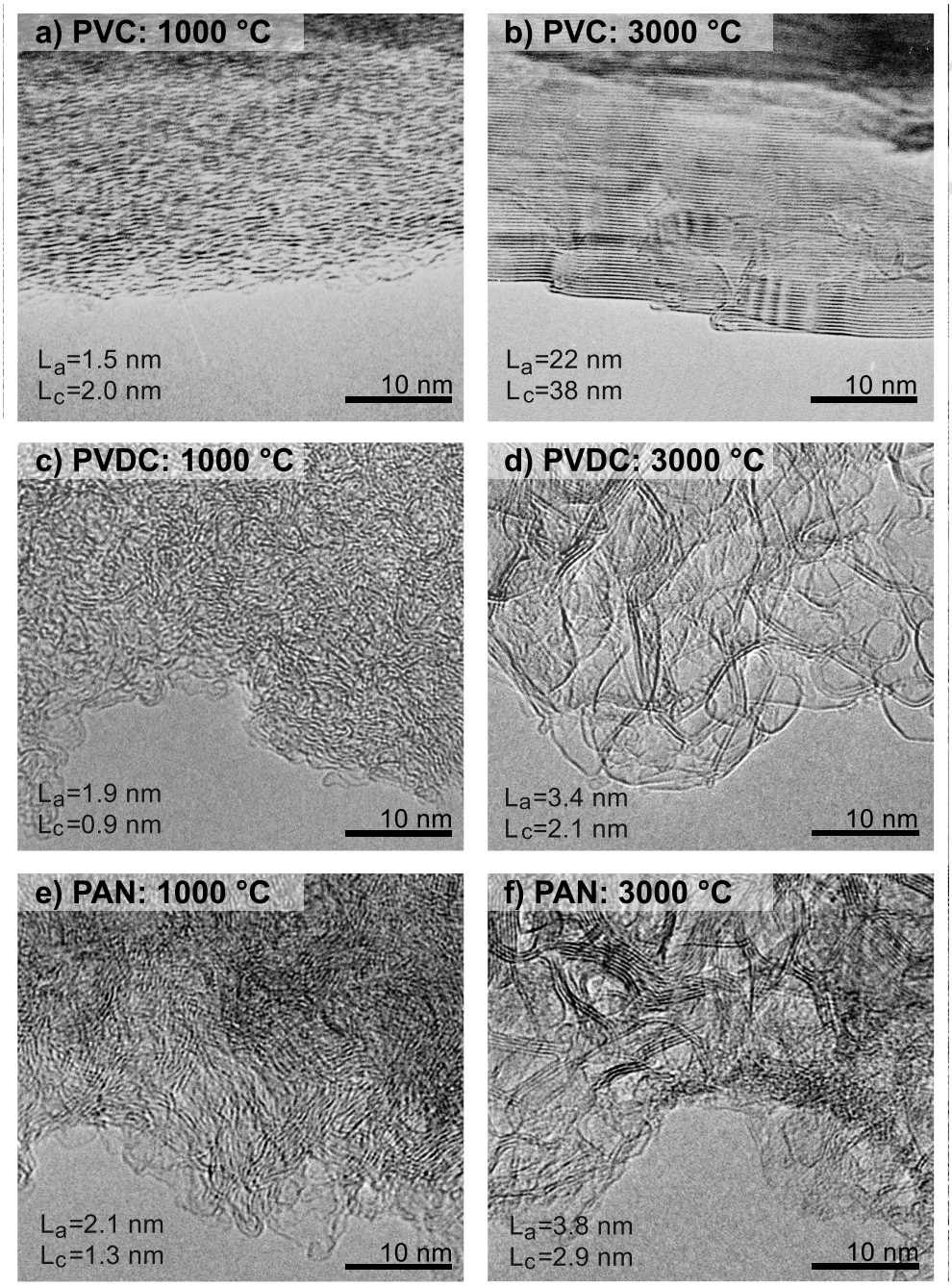

Figure 7: Transmission electron microscopy images of the three materials after carbonization at 1000 °C and HTT at 3000 °C. L_a is reported from the (100) peak and L_c is reported from the (002) peak.

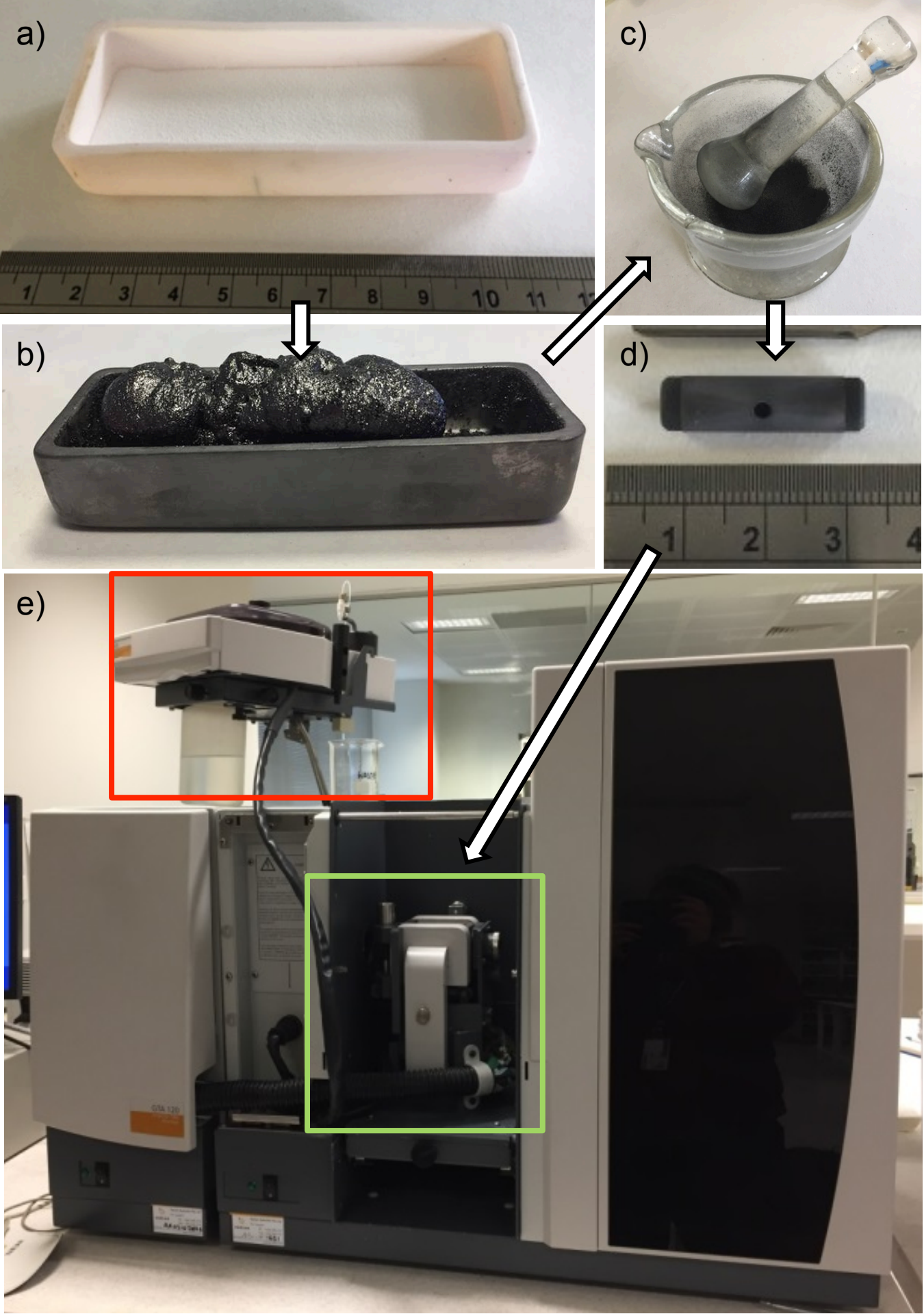
a)
c)
b)
d)
e)

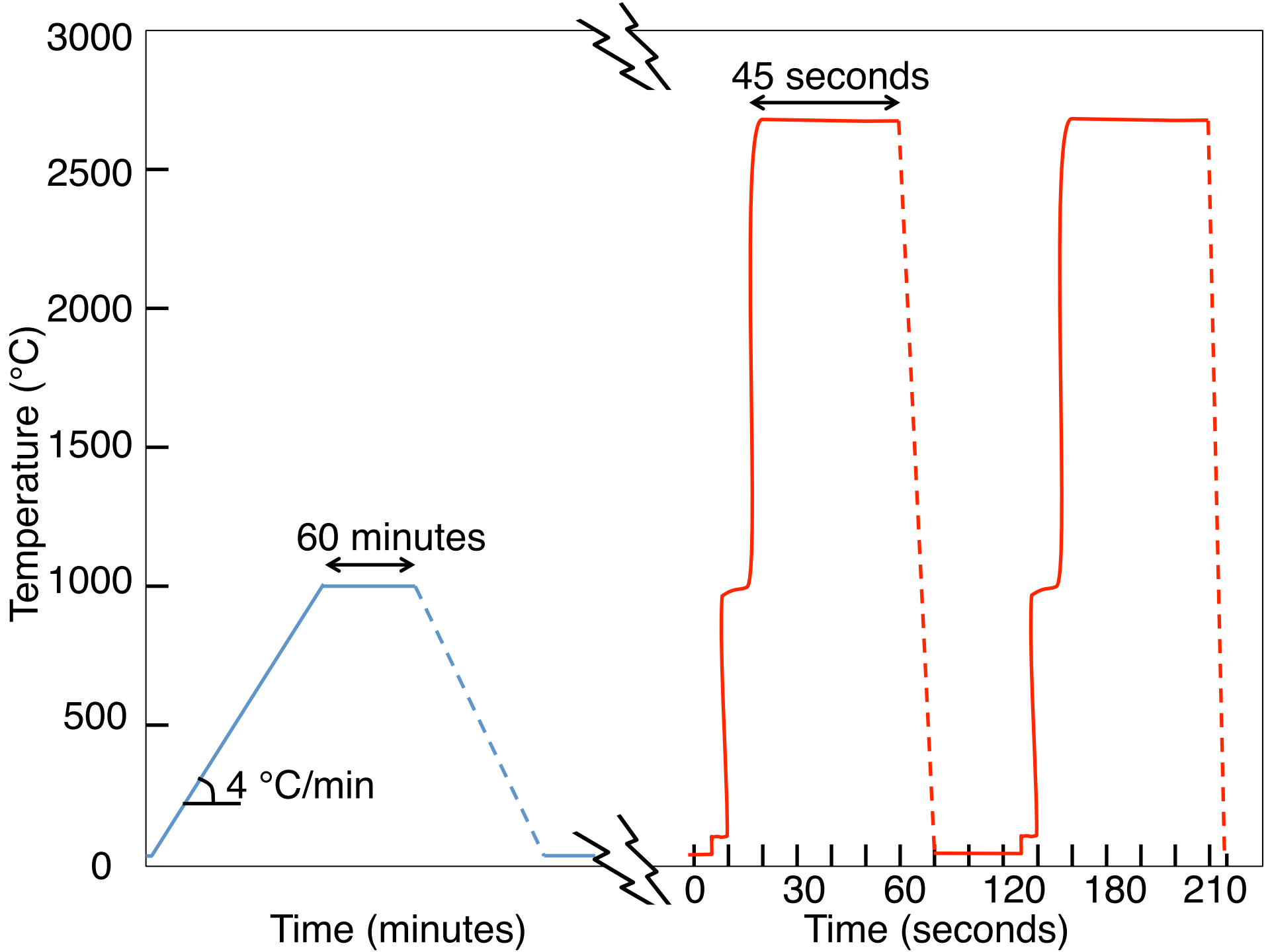
3000
2500
2000
1500
1000
500
0
Temperature (°C)
60 minutes
4 °C/min
45 seconds
0
30
60
120
180
210
Time (minutes)
Time (seconds)

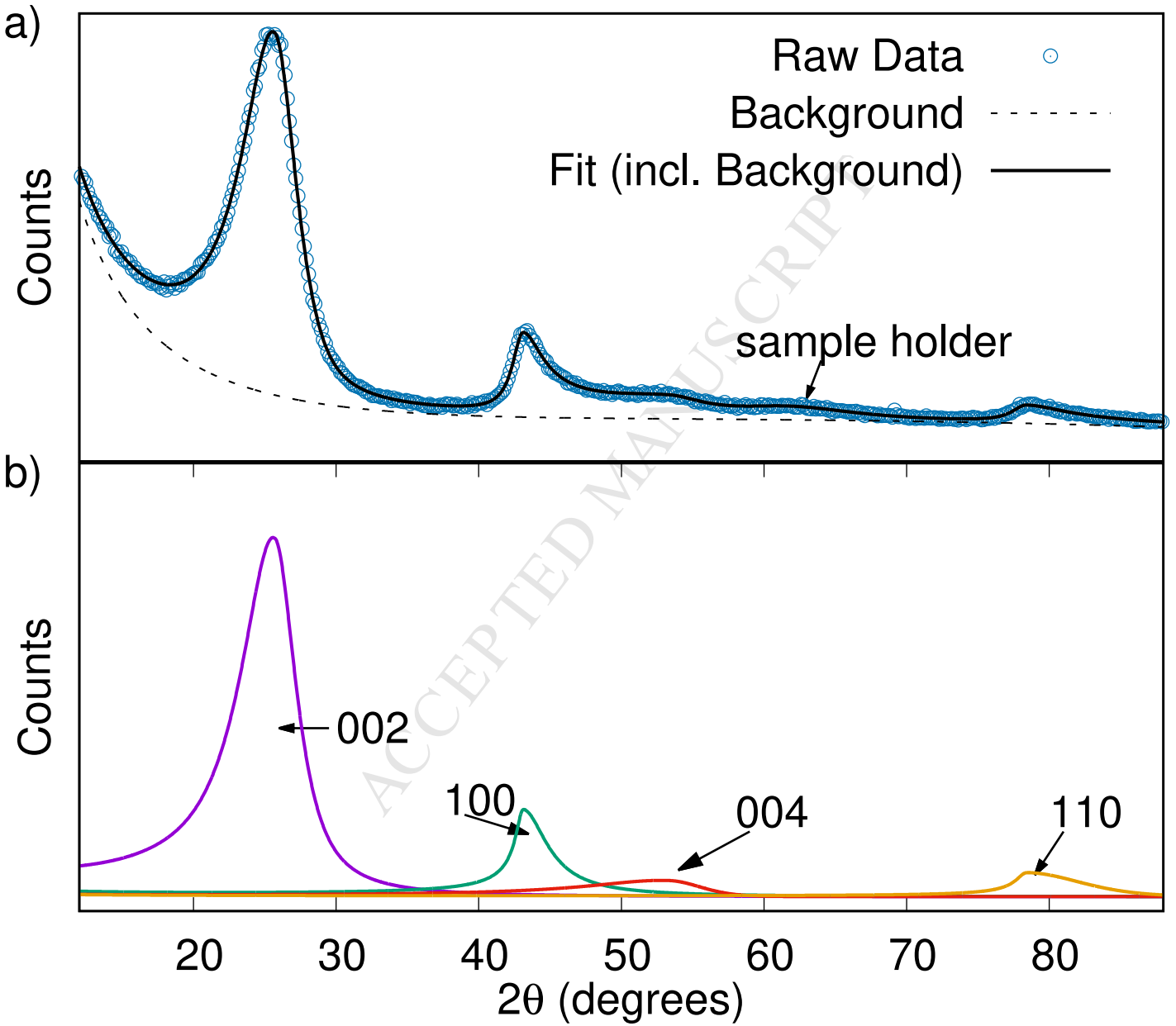

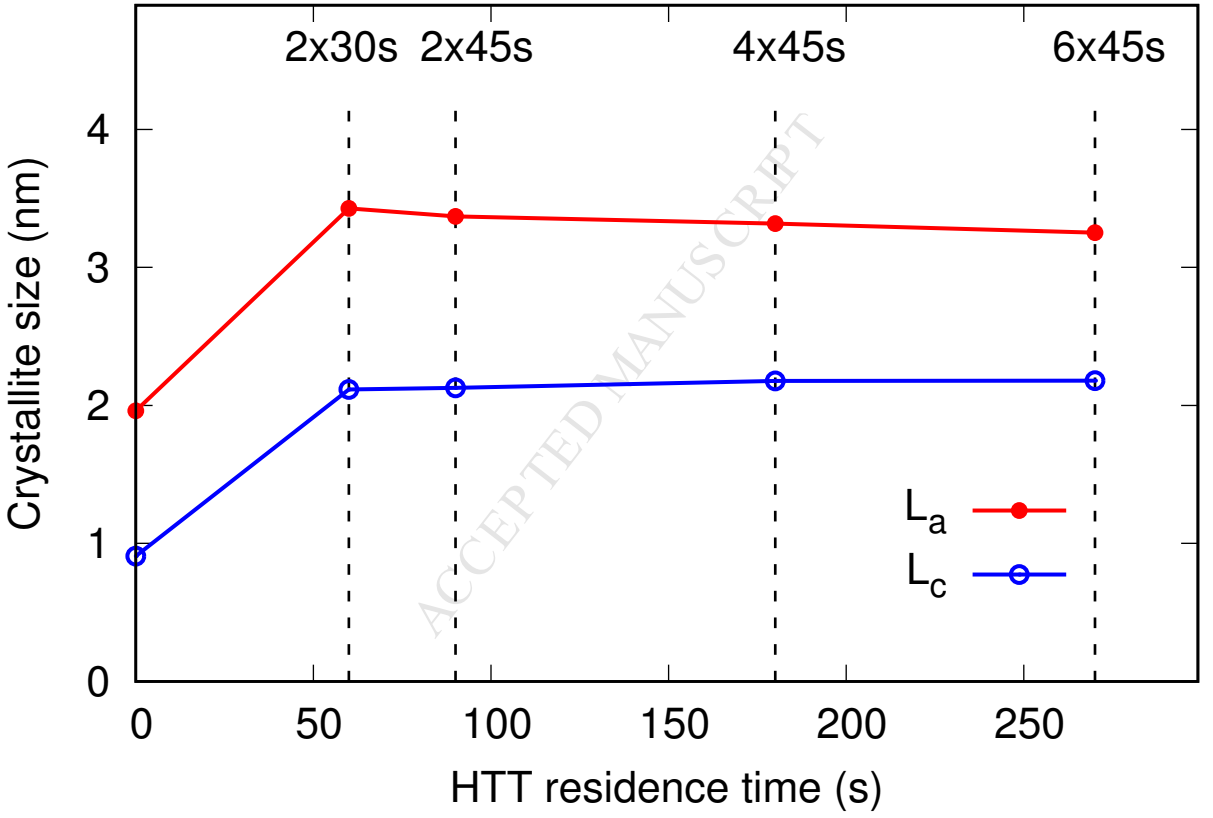

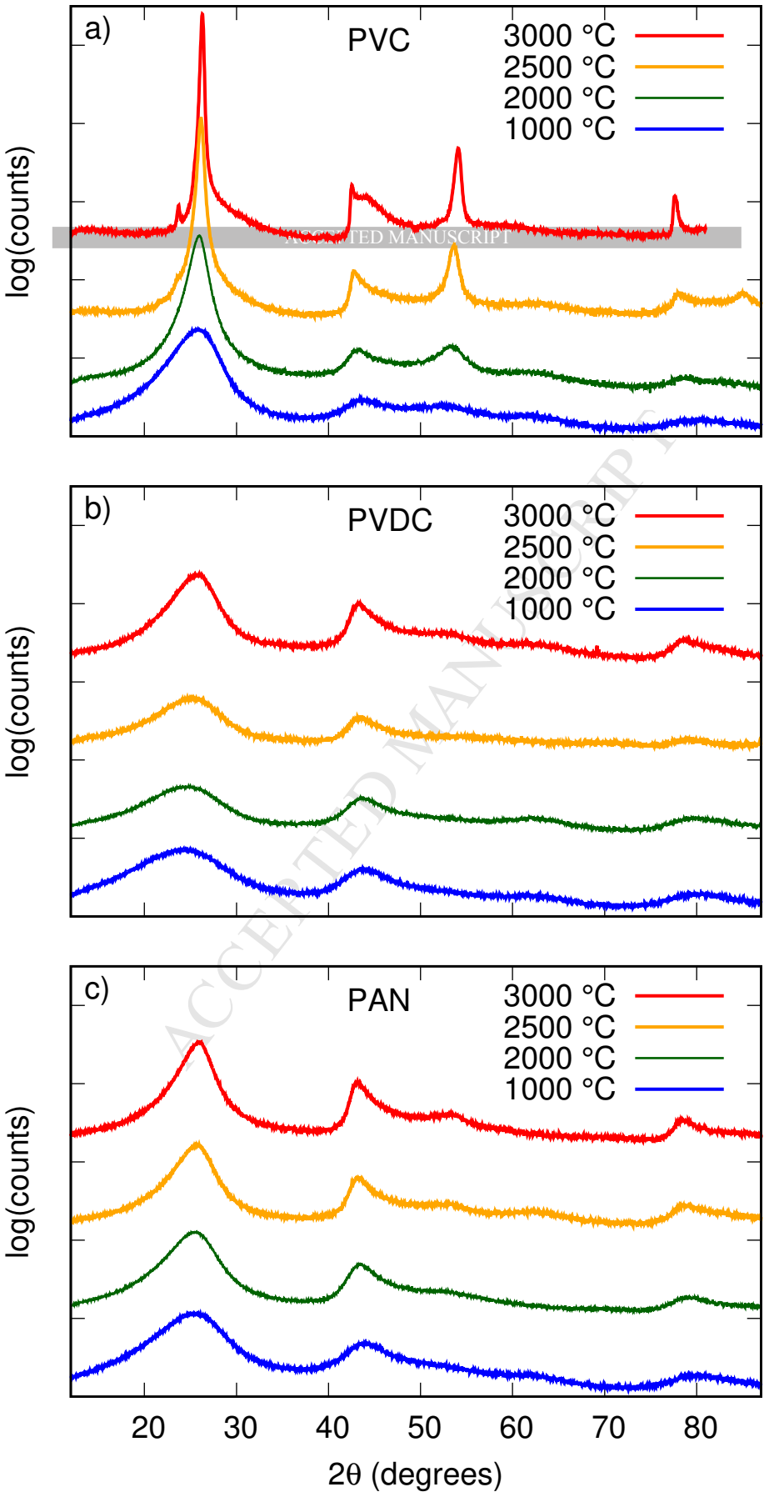

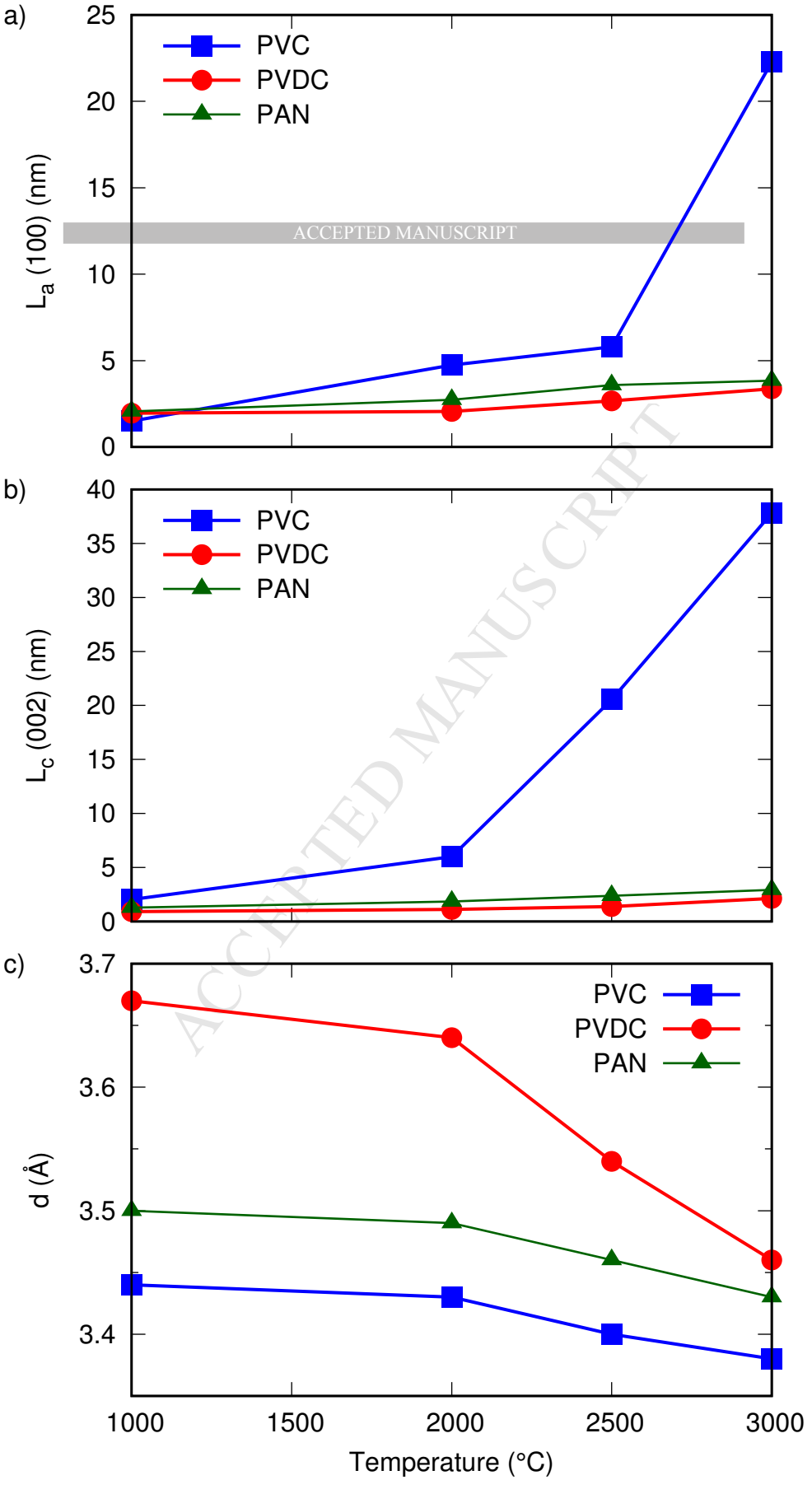

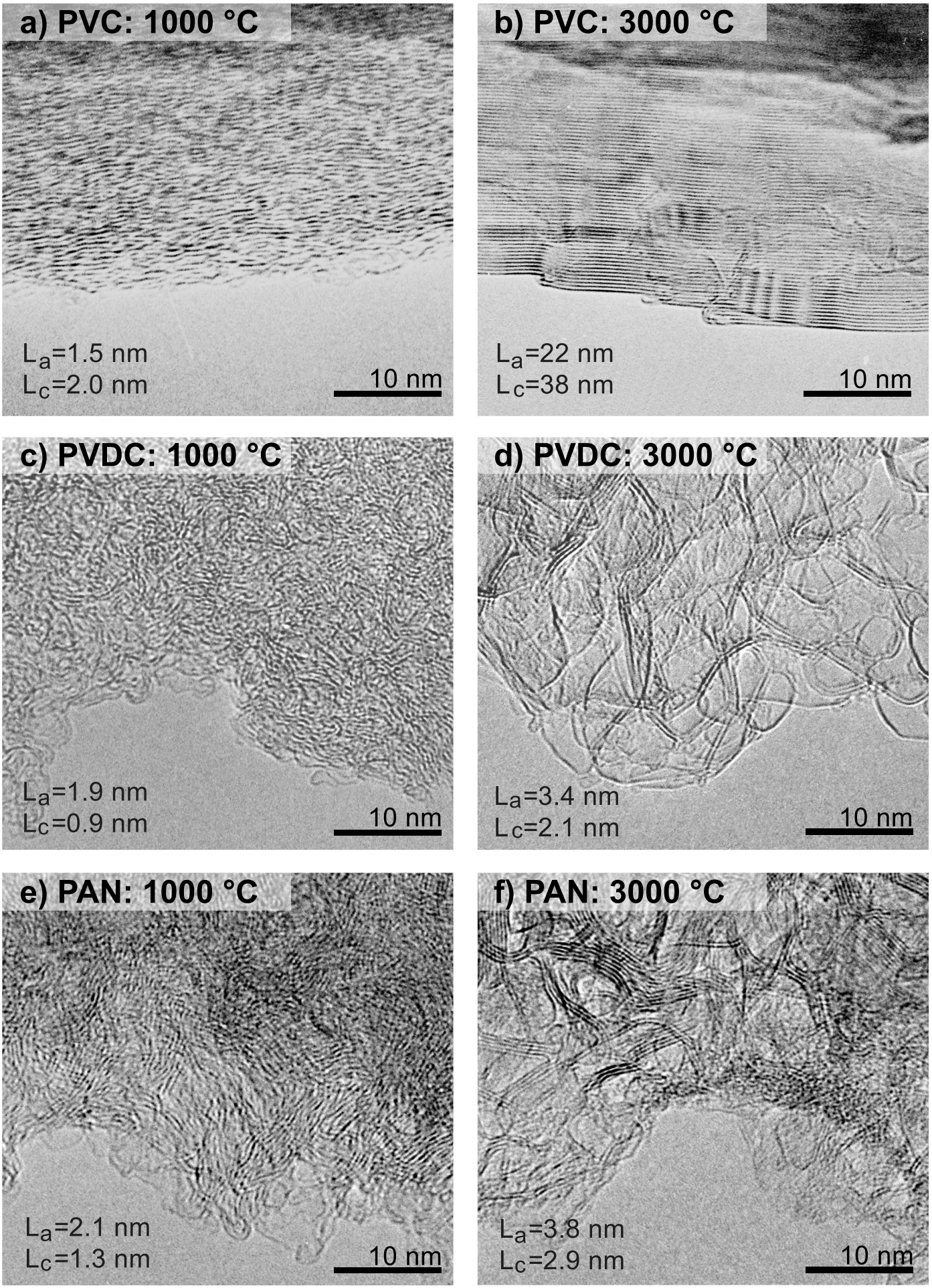
a) PVC: 1000 °C
L_a=1.5 nm
L_c=2.0 nm
10 nm
b) PVC: 3000 °C
L_a=22 nm
L_c=38 nm
10 nm
c) PVDC: 1000 °C
L_a=1.9 nm
L_c=0.9 nm
10 nm
d) PVDC: 3000 °C
L_a=3.4 nm
L_c=2.1 nm
10 nm
e) PAN: 1000 °C
L_a=2.1 nm
L_c=1.3 nm
10 nm
f) PAN: 3000 °C
L_a=3.8 nm
L_c=2.9 nm
10 nm